American Mineralogist, Volume 78, pages 68–74, 1993

Oriented chlorite lamellae in chromite from the Pedra Branca Mafic-Ultramafic Complex, Ceará, Brazil

MICHAEL E. FLEET, NÉLSON ANGELI,* YUANMING PAN
Department of Geology, University of Western Ontario, London, Ontario N6A 5B7, Canada

ABSTRACT

Chromite grains in chromitite from the Pedra Branca Mafic-Ultramafic Complex, Ceará, Brazil, contain lamellar inclusions of chlorite oriented parallel to {111}. The chromite grains have a core of aluminian chromite and a broad margin of ferrian chromite, formerly called "ferritchromit." The chlorite is a Cr-bearing IIb clinochlore, and the inclusions occur preferentially within "ferritchromit." The orientation relationship is $\mathbf{c}^*_{\text{chlorite}} \| [111]_{\text{chromite}}$, $\mathbf{a}_{\text{chlorite}} \| [\bar{h}h0]_{\text{chromite}}$, and $\mathbf{b}_{\text{chlorite}} \| [hh\bar{2}\bar{h}]_{\text{chromite}}$. This is equivalent to the orientation of chlorite-olivine intergrowths and corresponds to topotaxial sharing of a layer of closest-packed anions at the interface between the two phases. Because of the considerable misfit in the strain-free equivalent lattices, the interface structures in both chlorite-chromite and chlorite-olivine intergrowths may consist of an interlayer sheet (brucite layer) of H bonded to a layer of closest-packed O of the host substrate. Chloritization of the chromite was broadly contemporaneous with the alteration to "ferritchromit."

INTRODUCTION

Silicate mineral inclusions in chromite and chromian spinel are of current interest because of their possible bearing on the primary (early magmatic) origin of the nickel copper sulfides and platinum group minerals (PGMs) associated with chromitites (Talkington et al., 1984; Hulbert and Von Gruenewaldt, 1985; Lorand and Cotton, 1987; Thalhammer et al., 1990; McElduff and Stumpfl, 1991; Tarkian et al., 1991). Silicate phases reported as inclusions in chromite and chromian spinel include olivine, pyroxenes, amphiboles, serpentine, chlorite, and albite. The latter three phases are attributable to the effects of serpentinization and low-grade metamorphic alteration and are considered to be mostly alteration products of preexisting silicate inclusions (Thalhammer et al., 1990; McElduff and Stumpfl, 1991). In the Hochgrössen and Kraubath Ultramafic Massifs, Austria, chlorite within Cr-rich spinels occurs as lath-shaped, patchy or blocky grains and is generally associated with olivine and amphibole inclusions (Thalhammer et al., 1990). Serpentine is present either in association with chlorite or as lath-shaped inclusions in "ferritchromit." The chlorite there and in Cr-rich spinel of the Troodos Complex, Cyprus (McElduff and Stumpfl, 1991), is the Cr-rich variety formerly known as "kämmererite."

Cr fixed in chromite and chromian spinel by early-magmatic processes may be remobilized by subsolidus rock-fluid interaction (e.g., Pan and Fleet, 1989). A common intermediate alteration product of Cr-rich spinels during serpentinization and low-grade metamorphic alteration is the material "ferritchromit" (Weiser, 1967; Mihalik and Saager, 1968; Beeson and Jackson, 1969; Onyeagocha, 1974; Hamlyn, 1975; Ahmed and Hall, 1982; Wylie et al., 1987; Shen et al., 1988; Zakrzewski, 1989; Michailidis, 1990; Thalhammer et al., 1990). "Ferritchromit" is normally present as a continuous or discontinuous $Fe(Fe,Cr)_2O_4$-rich margin to a more $MgAl_2O_4$-rich core and is generally attributed to solid-state alteration or later overgrowth of preexisting chromite (e.g., Beeson and Jackson, 1969; Ulmer, 1974).

The present study reports on chlorite lamellae oriented parallel to {111} of chromite from the Pedra Branca Mafic-Ultramafic Complex, Brazil. This mineral intergrowth promotes discussion of the susceptibility of Cr-rich spinel, a refractory oxide phase, to intracrystalline replacement through the diffusion and infiltration of fluid species.

GEOLOGICAL SETTING

The Pedra Branca Mafic-Ultramafic Complex is located in the central region of Ceará State, northeast Brazil (Fig. 1). Geologically it belongs to the Borborema Structural Province (Almeida et al., 1981) and represents one of several portions of older crystalline basement, all characterized by a common tectonomagmatic orogeny of Upper Proterozoic age. The Pedra Branca Complex is part of the Tróia Median Massif in the Santa Quitéria structural block (Brito Neves, 1975), and comprises five mafic-ultramafic bodies (Mendes, Cedro, Esbarro, Curiu, and Trapiá), all mineralized in Cr. The present samples of chromitite are from the Esbarro body.

The country rocks in the southern part of the Tróia Median Massif are mainly gneisses (predominantly or-

* Present address: Departamento de Petrologia e Metalogenia da UNESP, 13500 Rio Claro, SP Brasil.

0003–004X/93/0102–0068$02.00

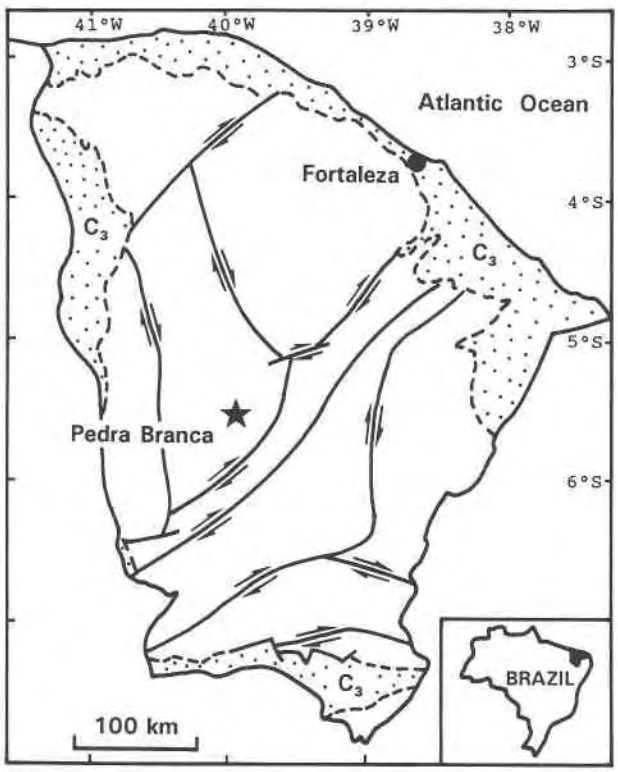

Fig. 1. Geological map of Ceará State, northeast Brazil, showing principal structural blocks of the Borborema Structural Province and locating the Pedra Branca Mafic-Ultramafic Complex within the Santa Quitéria structural block: C_3 is Phanerozoic sedimentary cover; see text; map simplified from DNPM (1983).

thogneiss, and locally migmatized) with small intercalations of quartzites, marbles, amphibolites, basic schists, and calc-silicate rocks (Angeli, 1982). The central part of the massif, which includes the Pedra Branca Complex, is mapped as "Reworked Archean Unit, the leptinites of Tróia" (DNPM, 1983). The country rocks are similar to those in the southern part of the massif with ages of 2.020 Ga, but older ages (2.700 Ga) also occur (Brito Neves, 1975). The Pedra Branca Mafic-Ultramafic Complex is presently interpreted as Archean in age.

Two metamorphic events are recorded in the Pedra Branca Mafic-Ultramafic Complex. The first was a regional metamorphism of medium to high grade and the second a more local, hydrothermal metamorphism of low grade with an age of 0.550 Ga (Brito Neves, 1975). The Esbarro body comprises mainly metaperidotites with minor mafic schists and serpentinites and contains several chromitite lenses within which cumulate texture is locally preserved, albeit in a generally chloritic matrix.

Materials and methods

The present study was made using two rock samples (PBR31, PBR32) from the principal chromitite lens of the Esbarro body, by thin- and polished-section optical petrography, electron microprobe analysis, and X-ray

Table 1. Average compositions of aluminian chromite core and "ferritchromit" margin

	Chromite $n = 14$	"Ferritchromit" $n = 7$
TiO_2 (wt%)	0.35(0.10)	0.74(0.13)
Al_2O_3	17.67(0.81)	5.73(0.52)
Cr_2O_3	43.16(0.99)	43.79(2.42)
Fe_2O_3*	8.37(1.19)	18.58(2.41)
FeO	22.87(0.54)	26.69(0.58)
MgO	7.64(0.34)	3.59(0.59)
MnO	0.51(0.24)	0.93(0.21)
ZnO	0.28(0.04)	0.31(0.08)
NiO	0.04(0.02)	0.17(0.06)
TOTAL	100.89(1.45)	100.53(1.12)
Chemical formulae calculated on the basis of 32 O		
Cr	8.84	9.81
Al	5.39	1.91
Fe^{3+}	1.63	3.96
Fe^{2+}	4.95	6.31
Ti	0.07	0.16
Mg	2.95	1.52
Mn	0.11	0.22
Zn	0.05	0.07
Ni	0.01	0.04
Σ (cations)	24.00	24.00
Cr/(Cr + Al)	0.62	0.84
Mg/(Mg + Fe)	0.37	0.19

Note: Wt% is weight percent.
* Fe_2O_3 calculated according to the method of Carmichael (1967); standard deviations in parentheses largely represent compositional variation.

Gandolfi and single-crystal diffraction procedures. Electron microprobe analyses were conducted with a Jeol JXA-8600 Superprobe electron microprobe at the University of Western Ontario, fitted with four automated wavelength-dispersive spectrometers, with an accelerating voltage of 15 kV, a beam current of 10 nA, and a beam diameter of 2–5 μm, with 20-s counts and the following minerals and synthetic glasses as standards: chromite, orthopyroxene, diopside, kaersutite, rhodonite, NiS, and ZnS. Matrix corrections were made with the Tracor Northern ZAF program.

Results

Both of the chromitite samples investigated consisted of hypidioblastic chromite grains with an approximately bimodal size distribution (1–2 mm and <1 mm in diameter) in a matrix of chlorite and minor albite and quartz. Sample PBR31 had about 45 modal% chromite and PBR32 about 35 modal %. In polished section, chromite grains were uniform in color (gray) and reflectivity in air, but a broad, light gray margin (of "ferritchromit," below) was discernible in oil. Anisotropy was very weak and restricted to very narrow zones of higher reflectivity (and oxidation) adjacent to late fractures and a few irregular patches in grain margins. Optical anisotropy was not associated with chromite at interfaces with included chlorite. By electron microprobe analysis (Table 1), large chromite grains had an irregular, patchy core of aluminian chromite (classification of Stevens, 1944) and a broad margin of ferrian chromite (Fig. 2A; Table 1). Smaller grains were largely of ferrian chromite (Fig. 2B). The aluminian chromite core may have too much Fe^{3+} to rep-

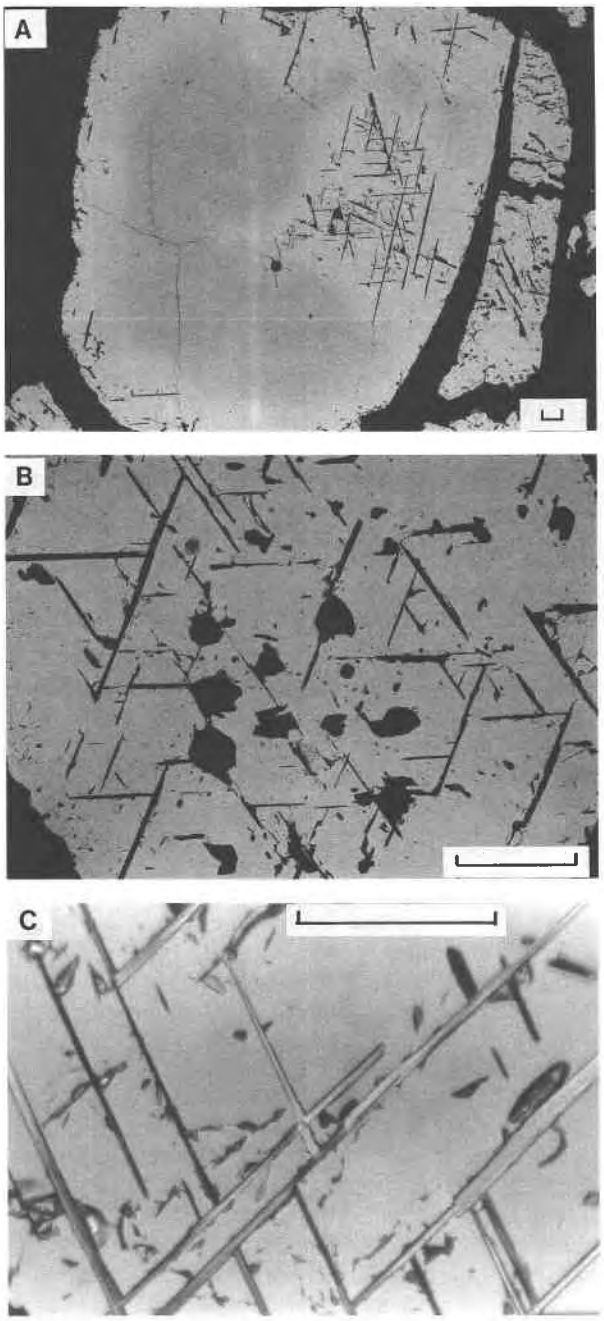

Fig. 2. Chlorite lamellar inclusions in chromite: (**A**) backscattered electron micrograph showing chlorite (dark) in "ferritchromit" margin (light gray) and irregular aluminian chromite core (medium-gray); scale bar is 0.1 mm; (**B**) backscattered electron micrograph showing four orientations of chlorite lamellae (dark; fourth orientation is in plane of section and represented by irregular patches) in smaller grain of "ferritchromit"; scale bar is 0.1 mm; (**C**) optical micrograph showing chlorite in "ferritchromit"; irregular dark areas are surface pits, oil, reflected and transmitted plane-polarized light; scale bar is 0.05 mm.

TABLE 2. Compositions of chlorite

Analysis	1	2	3	4	5
SiO_2 (wt%)	31.60	30.94	30.36	31.35	30.95
TiO_2	0.00	0.03	0.00	0.00	0.04
Al_2O_3	16.11	16.48	19.55	16.57	17.32
Cr_2O_3	2.96	2.94	1.63	2.39	1.71
FeO	3.11	3.33	2.60	2.94	3.62
NiO	0.16	0.17	0.13	0.14	0.14
MgO	33.99	33.60	33.10	34.15	33.35
TOTAL	87.94	87.51	87.36	87.54	87.31
Chemical formulae calculated on the basis of 28 O					
Si	5.96	5.87	5.71	5.92	5.88
$^{[4]}$Al	2.04	2.13	2.29	2.08	2.12
$^{[4]}\Sigma$ tet	8.00	8.00	8.00	8.00	8.00
$^{[6]}$Al	1.53	1.58	2.04	1.61	1.76
Ti	0.00	0.01	0.00	0.00	0.01
Cr	0.44	0.44	0.24	0.36	0.26
Fe	0.49	0.53	0.41	0.46	0.57
Ni	0.02	0.03	0.02	0.02	0.02
Mg	9.55	9.50	9.28	9.61	9.44
$^{[6]}\Sigma$ Oct	12.03	12.09	11.99	12.06	12.06

Note: 1 and 2 = lamellae in "ferritchromit" margin; 3 = aluminian chromite core; 4 = matrix close to chromite; 5 = matrix away from chromite.

resent the pristine primary composition. According to contemporary literature (e.g., Wylie et al., 1987; Zakrzewski, 1989; Michailidis, 1990), the ferrian chromite presumably corresponds to the intermediate alteration product formerly called "ferritchromit." Ferrian chromite compositions plot close to the Cr-rich limb of the solvus in the spinel-chromite-magnetite system (Loferski and Lipin, 1983; Zakrzewski, 1989).

Chlorite inclusions represented up to 5–10 modal% of smaller chromite grains (Figs. 2B, 2C) and were irregularly distributed in larger grains, being dominantly but not exclusively in areas of "ferritchromit" (Fig. 2A). The chlorite inclusions were present as lamellae oriented parallel to one of four directions that correspond to the four {111} planes of the host chromite (Fig. 1). Lamellar width varied up to 10 μm. In polished sections cut parallel to (111) of chromite, lamellae in all four orientations were visible (Fig. 2B). For sections cut rather thin, as in Figure 2B, lamellae in the fourth orientation, parallel to the plane of the section, appeared as rounded, six-sided, transparent windows within opaque chromite. In transverse section, chlorite lamellae were frequently terminated in ledges. By electron microprobe analysis (Table 2) the included chlorite is a chromian clinochlore, with 2–3 wt% Cr_2O_3 and corresponds to "kämmererite." The composition of lamellar chlorite in areas of "ferritchromit" was indistinguishable from that of chlorite in the rock matrix, but chlorite within the aluminian chromite core was relatively enriched in Al (Table 2). These observations on the composition of the chlorite inclusions within chromite from the Pedra Branca Complex are consistent with chlorite associated with chromite in other localities (Thalhammer et al., 1990; McElduff and Stumpfl, 1991).

A small grain fragment of chromite with numerous chlorite lamellae was removed from a thick section of sample PBR32 for X-ray diffraction study. From a Gandolfi power pattern, the unit-cell parameter of the chro-

TABLE 3. Comparative *h0l* reflection intensities for chlorites

hkl	1 Pedra Branca	2 Ia-4	3 IIb
208	8	47	2½
207	—	27	—
206	3	161	1½
205	3	28	2½
204	9	152	6
203	—	29	—
202	5	199	4
201	10	34	8
200	—	108	—
$20\bar{1}$	<1	43	1½
$20\bar{2}$	6	69	5
$20\bar{3}$	8	23	7
$20\bar{4}$	*	62	4
$20\bar{5}$	1	55	1½
$20\bar{6}$	3	53	2½
$20\bar{7}$	—	74	½
$20\bar{8}$	6	120	3

Note: (Compare with Fig. 3.) (1) Pedra Branca, oriented inclusions in "ferritchromit", estimated visually from precession film; (2) Cr-rich chlorite with Ia-4 stacking structure, observed structure factors (Brown and Bailey, 1963); (3) Chlorite with common IIb stacking structure, powder pattern (labeled A in Table 1.22 of Bailey, 1980).

* Obscured by white radiation diffraction streak of host chromite.

mite was 8.365(7) Å, consistent with the present composition of "ferritchromit" (Deer et al., 1962, their Fig. 6). X-ray precession study of this grain fragment revealed weak reflections of chlorite (Fig. 3) with 20*l* reflection intensities (Table 3) consistent with the IIb stacking structure (Bailey, 1980). This is the most common stacking structure of natural chlorites, being present in 80% of the 303 chlorites examined by Bailey and Brown (1962) and differing from the triclinic one-layer Ia-4 structure of the "kämmererite" with 9.3 wt% Cr_2O_3 that was investigated by Brown and Bailey (1963).

The precession films (Fig. 3) revealed that the chlorite reciprocal lattice was oriented relative to that of the chromite matrix, with $00l_{\text{chlorite}} \| hhh_{\text{chromite}}$, $0k0_{\text{chlorite}} \| hh\bar{2}h_{\text{chromite}}$, and $h00_{\text{chlorite}} \wedge \bar{h}h0_{\text{chromite}} \approx 7°$, and was repeated by threefold rotation about hhh_{chromite}. Most interestingly, any given $[11\bar{2}]$ zero-level precession film of chromite reveals only one orientation of the chlorite reciprocal lattice. Thus, the reciprocal lattice of the intergrowth phase is not twinned by twofold rotation about hhh_{chromite}.

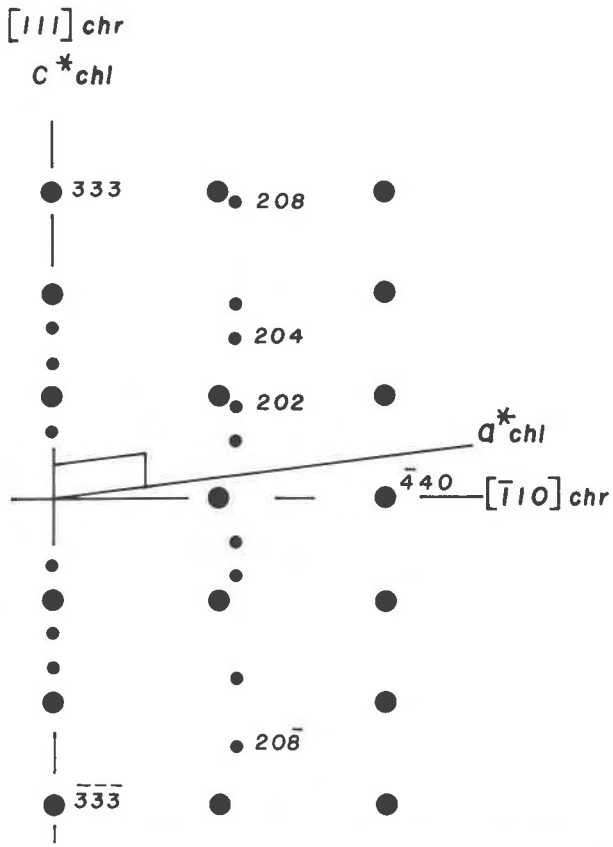

Fig. 3. Interpretation of part of precession photograph of chromite grain with chlorite lamellar inclusions: Mo$K\alpha$; $\bar{\mu} = 25°$; zero level; chr = chromite; chl = chlorite; precession axis is $[11\bar{2}]$; large circles = chromite reflections; small circles = chlorite reflections; see Table 3.

DISCUSSION

Chlorite-chromite intergrowth

Chlorite in chromitite from the Pedra Branca Mafic-Ultramafic Complex is a Cr-bearing clinochlore corresponding to the variety "kämmererite." Lamellar inclusions of chlorite have a preferred crystallographic orientation with chromite host crystals, with $\mathbf{c}^*_{\text{chlorite}} \| [111]_{\text{chromite}}$, $\mathbf{a}_{\text{chlorite}} \| [\bar{h}h0]_{\text{chromite}}$, and $\mathbf{b}_{\text{chlorite}} \| [hh\bar{2}h]_{\text{chromite}}$. Also, of course, $(001)_{\text{chlorite}} \| (111)_{\text{chromite}}$, corresponding to parallelism of the layers of closest-packed O atoms or OH groups in the two structures. Because there are three chlorite orientations for each [111] direction of chromite, there must be a maximum of 12 individual chlorite orientations in each grain of chromite.

The present chlorite lamellae are therefore analogous to the familiar {111} exsolution-oxidation lamellae of ilmenite-hematite solid solution in titanomagnetite (e.g., Haggerty, 1976), where the control of layers of closest-packed O atoms on interface orientation is paramount. Chlorite and interlayer smectite-chlorite also exhibit oriented replacement of olivine, with $\mathbf{c}^*_{\text{chlorite}} \| \mathbf{a}_{\text{olivine}}$, and $[100]_{\text{chlorite}} \| \mathbf{b}$, [013], $[01\bar{3}]_{\text{olivine}}$ (Brindley and Ali, 1950; Brown and Stephen, 1959; Fleet and MacRae, 1975). Once again, the layers of closest-packed O atoms or OH groups in chlorite are parallel to closest-packed layers in the host crystals. However, in the ideal olivine structure, the O layers are hexagonal closest packed (ABABABA. . . . layer sequence) whereas in the spinel structure they are cubic closest packed (ABCABCAB. . . .).

As discussed in Fleet (1982) and Fleet and Arima (1985), the dominant factor controlling the shape and orientation of crystalline precipitates and replacement products in minerals is minimization of interfacial energy. Thus, oriented inclusions tend to have either a topotactic (syntactic) relationship with the matrix phase or an orientation that minimizes the dimensional misfit between the strain-free lattices at the phase boundary. As

TABLE 4. Derived unit-cell edges (Å) of equivalent orthorhombic lattices of chlorite, olivine, and chromite

	Chlorite	Forsterite	Chromite
a'	6.20 ($=\frac{2}{3}b$)	5.98 ($=c$)	5.91 ($=2d_{220}$)
b'	10.74 ($=2a$)	10.20 ($=b$)	10.24 ($=6d_{22\bar{4}}$)
c'	14.08 ($=d_{001}$)	14.27 ($=3a$)	14.49 ($=3d_{111}$)
V (Å^3)	937.8	870.0	878.0
		Cell contents	
O cations	16	24	24
T cations	10.7	12	12
Anions	48	48	48

Note: Compare with Figures 4 and 5.

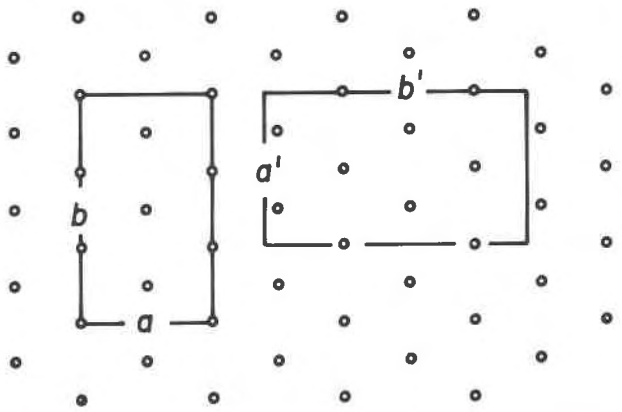

Fig. 4. Closest-packed net representing layer of O and OH anions, showing outline of chlorite unit cell (**a**, **b**) and defining equivalent orthorhombic unit cell (**a**′, **b**′) for chlorite, olivine, and chromite; there are three equivalent orientations of each unit cell on the closest-packed substrate; see Table 4 and text.

defined in Fleet and Arima (1985), topotaxy involves a shared structural element, and therefore topotactic phase boundaries are usually rational planes. Their orientation is independent of the precise values of the strain-free lattice parameters. On the other hand, phase boundaries defined by minimization of lattice misfit are, in general, irrational, and their orientation is sensitive to change in lattice parameters through change in temperature, pressure, composition, and so on. Dimensional (lattice) misfit boundaries are more characteristically associated with a matrix phase of low symmetry (triclinic and monoclinic), whereas topotactic boundaries are associated with a matrix phase of higher symmetry.

Thus, magnetite inclusions in augite were observed to have coincident phase boundaries (Fleet et al., 1980) and to be completely analogous to the more familiar intergrowths of isomorphous monoclinic chain silicates (e.g., Robinson et al., 1977). However, where the matrix phase is cubic, as in the present chlorite-chromite intergrowth, previous experience suggests that the intergrowth orientation should be controlled by topotaxy. That this is the case is readily demonstrated by the lack of close dimensional correspondence between equivalent lattices of the two phases and by the absence of lattice rotation (Fig. 3).

Analysis of dimensional correspondence begins with the recognition of equivalent lattices for the two intergrown phases, derived on the basis of a common structural feature (Table 4, Fig. 4). Coincident and optimal phase boundaries have indices (*hkl*) common to both lattices (Fleet, 1982). For the pseudomorphous replacement of olivine by chlorite (as above), the olivine and chlorite structures share layers of closest-packed O atoms. In the olivine structure, layers of approximate closest-packed O atoms are parallel to (100), and in the chlorite structure, layers of closest-packed O atoms or OH groups parallel to (001) enclose and define the octahedral cation layer within the 2:1 layer, and the brucite layer in the interlayer position. There are therefore three possible orientations of chlorite on an olivine substrate (Fig. 4). However, there is a considerable misfit in the strain-free equivalent lattices at the interface, equal to +9.2 area% (Table 4). This misfit could be compensated by coherency stresses during nucleation of the chlorite replacement phase, but ultimately the two structures would have to relax. Therefore the structure at the interface most likely consists of an interlayer sheet (brucite layer) on an olivine substrate. The misfit is then compensated by sliding an OH layer, with its H bonding, along the layer of closest-packed O atoms associated with the olivine side of the interface.

Turning to the present chlorite-chromite intergrowth, the equivalent orthorhombic unit cell for chromite is closely comparable to that of olivine (Table 4, Fig. 4). The structural correspondence is similar to that for the chlorite-olivine intergrowth and gives the observed orientation relationship $\mathbf{c}^*_{\text{chlorite}} \| [111]_{\text{chromite}}$, $\mathbf{a}_{\text{chlorite}} \| [\bar{h}h0]_{\text{chromite}}$, and $\mathbf{b}_{\text{chlorite}} \| [hh\bar{2}\bar{h}]_{\text{chromite}}$. Similarly to the chlorite-olivine intergrowth, the interface structure most likely consists of an interlayer sheet (brucite layer) on a mixed tetrahedral and octahedral {111} layer of the chromite structure, as indicated in Figure 5, so that the lattice misfit may be compensated by sliding a H-bonding layer over a layer of closest-packed O atoms.

In summary, the interface in the chlorite-chromite intergrowth is neither a coincident boundary nor an optimal one (cf., Fleet, 1982). The interface orientation is controlled by topotaxy, but the interface is not coherent. Layers of closest-packed ligand atoms are not in registry out of the plane of the interface, and the parallelism of the closest-packed layers most probably results from the accommodating nature of the H bonding associated with the interlayer sheet.

In contrast to oriented chlorite lamellae in chromite, cubic phases intimately intergrown with spinels commonly exhibit a {100} orientation (e.g., ulvöspinel in pleonaste spinel and titanomagnetite, Haggerty, 1976; Frost and Gai, 1980; Ni_2TiO_4 (spinel) in NiO (rocksalt), De Graef et al., 1985). The {100} intergrowth orientation is clearly not related to topotaxy through the sharing of layers of closest-packed O atoms. Also, as in all cubic-cubic intergrowths, the lattice misfit is isotropic and does not influence intergrowth orientation. However, intergrowth orientation could well be controlled by minimi-

zation of the elastic strain energy required to maintain coherence of the phase boundaries during nucleation of the lamellar structures (e.g., Cahn, 1968). Thus precipitates would tend to follow elastically soft planes and to be oriented to the direction of the minimum in Young's modulus of the matrix phase. For cubic crystals, the elastic anisotropy factor (A) is given by $2c_{44}/(c_{11} - c_{12})$, where the c_{ij} values are the elastic stiffness constants (e.g., Newnham, 1975). When $A > 1$, as it is in spinel (2.43), magnetite (1.12), chromite (1.31), and MgO (1.51), the host crystal is most compliant along [100] and stiffest along [111], and therefore cubic-cubic intergrowths have a {100} orientation.

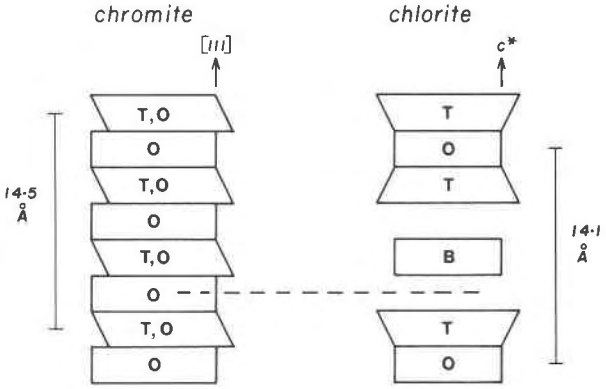

Fig. 5. Schematic representations of stacking structures of chromite and one-layer chlorite, defining equivalent stacking sequences and suggesting a possible structure for the chlorite-chromite interface (by translation of chlorite structure along broken line); T,O = layer of mixed tetrahedral and octahedral cations; O = octahedral cations; T = tetrahedral cations; B = brucite layer (interlayer sheet of octahedral cations); 14.5 Å is the translation distance along [111] of chromite, the body diagonal of the cubic unit cell.

Replacement processes in chromite

The chromitite from the Pedra Branca Mafic-Ultramafic Complex has been extensively modified by rock-fluid processes under low-grade conditions, presumably during the event 0.550 Ga (Brito Neves, 1975). Our observations (Fig. 2A, Tables 1, 2) are consistent with an origin for "ferritchromit" by solid state metasomatic replacement of preexisting chromite, as in Beeson and Jackson (1969) and Shen et al. (1988), along with extensive resorption of chromite by the rock matrix. The compositions of "ferritchromit" areas of chromite grains largely represent progressive replacement of the $MgAl_2O_4$ component by $FeFe_2O_4$ (Table 1). The extensive interaction between chromite grains and the rock matrix, the equilibration of chlorite included in "ferritchromit" with that in the matrix, and the increase in the Al content of chlorite included in aluminian chromite core areas all point to the broadly contemporaneous development of "ferritchromit" and lamellar chlorite (cf. Evans and Frost, 1975). Following the present discussion on the control of intergrowth structure on the orientation of chlorite lamellae, the intimate interleaving of chlorite and serpentine in the matrix of the Heng-Chun chromitite (Shen et al., 1988) is unlikely to have been inherited from the proposed {100} intergrowth of RO (rocksalt) and R_3O_4 (spinel) phases (where R = Fe, Cr, Mg, and Al) in the "ferritchromit." Moreover, nonstoichiometry of "ferritchromit" consistent with ($RO + R_3O_4$) was not demonstrated in this earlier study; rather the electron microprobe analyses in Table 1 of Shen et al. (1988) have not been renormalized to 32 O atoms after estimation of Fe^{3+} content.

As in the case of many lamellae of ilmenite-hematite solid solution in spinels, the present chlorite lamellae grew by the diffusion of constituents through the chromite crystals. The lamellae nucleated in the interior of the chromite grains and not at the grain boundaries. For constituents of the chlorite lamellae, whether we are dealing with lattice diffusion or a (faster) hopping migration along planar defects is unknown, but the aluminian chromite-"ferritchromit" interface (Fig. 2A) does appear to be consistent with lattice diffusion, at least as observed at the resolution of the backscattered electron image. Also, the diffusion of Mg and Al away from the aluminian chromite can account for their contents in lamellar chlorite. However, other mechanisms proposed for the formation of "ferritchromit" at other localities (see Wylie et al., 1987) may have contributed in the present case.

The refractory nature of inclusions in chromian spinel and chromitite is certainly suspect, and reported trapping of inclusions during crystal growth of chromite has to be confirmed by consistency with expected phase relations. Single-phase inclusions of sulfides (chalcopyrite, pentlandite, etc.) and of many platinum group minerals just do not pass this stringent test (cf. Hulbert and Von Gruenewaldt, 1985; Thalhammer et al., 1990; McElduff and Stumpfl, 1991; Stone et al., 1989; Fleet et al., 1991).

Acknowledgments

We thank two journal referees for helpful comments, R.L. Barnett and D.M. Kingston for assistance with electron microprobe analysis, and FAPESP (Brazil) for financial support to N.A. This study was supported by a Natural Sciences and Engineering Research Council of Canada operating grant to M.E.F.

References cited

Ahmed, Z., and Hall, A. (1982) Nickeliferous opaque minerals associated with chromite alteration in the Sakhakot-qila complex, Pakistan, and their compositional variation. Lithos, 15, 39–47.

Almeida, F.F.M., de, Hasui, Y., de Brito Neves, B.B., and Fuck, R.A. (1981) Brazilian structural provinces: An introduction. Earth Science Reviews, 17, 1–29.

Angeli, N. (1982) Geology of southern portion of Tróia Massif, Ceará. 32nd Brazilian Geological Congress, 1, 294–307 (in Portuguese).

Bailey, S.W. (1980) Structures of layer silicates. In G.W. Brindley and G. Brown, Eds., Crystal structures of clay minerals and their identification. Mineralogical Society Monograph, 5, 1–123.

Bailey, S.W., and Brown, B.E. (1962) Chlorite polytypism. I. Regular and semi-random one-layer structures. American Mineralogist, 47, 819–850.

Beeson, M.H., and Jackson, E.D. (1969) Chemical composition of altered

chromites from the Stillwater Complex, Montana. American Mineralogist, 54, 1084–1100.

Brindley, G.W., and Ali, S.Z. (1950) X-ray study of thermal transformations in some magnesium chlorite minerals. Acta Crystallographica, 3, 25–30.

Brito Neves, B.B. de (1975) Geotectonic regionalization of Northeastern Precambrian, 198 p. Ph.D. thesis, University of São Paolo (in Portuguese).

Brown, B.E., and Bailey, S.W. (1963) Chlorite polytypism. II. Crystal structure of a one-layer Cr-chlorite. American Mineralogist, 48, 42–61.

Brown, G., and Stephen, I. (1959) A structural study of iddingsite from New South Wales, Australia. American Mineralogist, 44, 251–260.

Cahn, J.W. (1968) Spinodal decomposition. Transactions of the Metallurgical Society of AIME, 242, 166–180.

Carmichael, I.S.E. (1967) The iron-titanium oxides of salic volcanic rocks and their associated ferromagnesium minerals. Contributions to Mineralogy and Petrology, 14, 36–64.

Deer, W.A., Howie, R.A., and Zussman, J. (1962) Rock-forming minerals, vol. 5: Non-silicates, 371 p. Longman, London.

De Graef, M., Seinen, P.A., and Ijdo, D.J.W. (1985) Electron microscopic study of the system NiO-TiO_2. I. $Ni_{2(1+x)}Ti_{1-x}O_4$ compounds. Journal of Solid State Chemistry, 58, 357–367.

DNPM (1983) Brazilian National Department of Mineral Production Geological Map of Ceará, Scale 1:500,000 (in Portuguese).

Evans, B.W., and Frost, B.R. (1975) Chrome-spinel in progressive metamorphism: A preliminary analysis. Geochimica et Cosmochimica Acta, 39, 959–972.

Fleet, M.E. (1982) Orientation of phase and domain boundaries in crystalline solids. American Mineralogist, 67, 926–936.

Fleet, M.E., and Arima, M. (1985) Oriented hematite inclusions in sillimanite. American Mineralogist, 70, 1232–1237.

Fleet, M.E., and MacRae, N.D. (1975) A spinifex rock from Munro Township, Ontario. Canadian Journal of Earth Sciences, 12, 929–939.

Fleet, M.E., Bilcox, G.A., and Barnett, R.L. (1980) Oriented magnetite inclusions in pyroxenes from the Grenville province. Canadian Mineralogist, 18, 89–99.

Fleet, M.E., Tronnes, R.G., and Stone, W.E. (1991) Partitioning of platinum group elements in the Fe-O-S system to 11 GPa and their fractionation in the mantle and meteorites. Journal of Geophysical Research, 96, 21949–21958.

Frost, R., and Gai, P.L. (1980) Oxidation reactions in natural Fe-Ti oxide spinels. Acta Crystallographica, 36A, 678–682.

Haggerty, S.E. (1976) Opaque mineral oxides in terrestrial igneous rocks. In D. Rumble III, Ed., Oxide minerals. Reviews in Mineralogy, 3, Hg101–Hg300.

Hamlyn, P.R. (1975) Chromite alteration in the Panton Sill, East Kimberley region, W. Australia. Mineralogical Magazine, 40, 181–192.

Hulbert, L.J., and Von Gruenewaldt, G. (1985) Textural and compositional features of chromite in the Lower and Critical zones of the Bushveld complex south of Potgeitersrus. Economic Geology, 80, 872–895.

Loferski, P.J., and Lipin, B.R. (1983) Exsolution in metamorphosed chromite from the Red Lodge district, Montana. American Mineralogist, 68, 777–789.

Lorand, J.P., and Cotton, J.Y. (1987) Na-Ti-Zr-H_2O-rich mineral inclusions indicating postcumulus chrome-spinel dissolution and recrystallization in the Western Laouni mafic intrusion, Algeria. Contributions to Mineralogy and Petrology, 97, 251–263.

McElduff, B., and Stumpfl, E.F. (1991) The chromite deposits of the Troodos Complex, Cyprus: Evidence for the role of a fluid phase accompanying chromite formation. Mineralium Deposita, 26, 307–318.

Michailidis, K.M. (1990) Zoned chromites with high Mn-contents in the Fe-Ni-Cr-laterite ore deposits from the Edessa area in Northern Greece. Mineralium Deposita, 25, 190–197.

Mihalik, P., and Saager, R. (1968) Chromite grains showing altered borders from the basal reef, Witwatersrand system. American Mineralogist, 53, 1543–1550.

Newnham, R.E. (1975) Structure-property relations, 234 p. Springer-Verlag, Berlin.

Onyeagocha, A.C. (1974) Alteration of chromite from the Twin Sisters Dunite, Washington. American Mineralogist, 59, 608–612.

Pan, Y., and Fleet, M.E. (1989) Cr-rich calc-silicates from the Hemlo area, Ontario. Canadian Mineralogist, 27, 565–577.

Robinson, P., Ross, M., Nord, G.L., Jr., Smyth, J.R., and Jaffe, H.W. (1977) Exsolution lamellae in augite and pigeonite: Fossil indicators of lattice parameters at high temperature and pressure. American Mineralogist, 62, 857–873.

Shen, P., Hwang, S.-L., Chu, H.-T., and Jeng, R.-C. (1988) STEM study of "ferritchromit" from the Heng-Chun chromitite. American Mineralogist, 73, 383–388.

Stevens, R.E. (1944) Composition of some chromites of the Western hemisphere. American Mineralogist, 29, 1–34.

Stone, W.E., Fleet, M.E., and MacRae, N.D. (1989) Two-phase nickeliferous monosulfide solid solution (mss) in megacrysts from Mount Shasta, California: A natural laboratory for nickel-copper sulfides. American Mineralogist, 74, 981–993.

Talkington, R.W., Watkinson, D.H., Whittaker, P.J., and Jones, P.C. (1984) Platinum-group minerals and other solid inclusions in chromite of ophiolite complexes: Occurrence and petrological significance. Tschermaks' mineralogische petrographische Mitteilungen, 32, 285–301.

Tarkian, M., Naidenova, E., and Zhelyaskova-Panayotova, M. (1991) Platinum-group minerals in chromitites from the Eastern Rhodope Ultramafic Complex, Bulgaria. Mineralogy and Petrology, 44, 73–87.

Thalhammer, O.A.R., Prochaska, W., and Mühlhans, H.W. (1990) Solid inclusions in chrome-spinels and platinum group element concentrations from the Hochgrössen and Kraubath Ultramafic Massifs (Austria). Contributions to Mineralogy and Petrology, 105, 66–80.

Ulmer, G.C. (1974) Alteration of chromite during serpentinization in the Pennsylvania-Maryland district. American Mineralogist, 59, 1236–1241.

Weiser, T. (1967) Untersuchungen mit der Electronenmikrosonde über die Zuzammensetzung von Chromiten. Neues Jahrbuch für Mineralogie Abhandlungen, 107, 113–143.

Wylie, A.G., Candela, P.A., and Burke, T.M. (1987) Compositional zoning in unusual Zn-rich chromite from the Sykesville district of Maryland and its bearing on the origin of "ferritchromit". American Mineralogist, 72, 413–422.

Zakrzewski, M.A. (1989) Chromian spinels from Kusså, Bergslagen, Sweden. American Mineralogist, 74, 448–455.

Manuscript received March 5, 1992
Manuscript accepted August 23, 1992